DEVELOPMENTAL BIOLOGY 177, 449–462 (1996)
ARTICLE NO. 0177

Expression of Zebrafish *connexin43.4* in the and Mutant *no tail* Embryos

J. J. Essner,* J. G. Laing,† E. C. Beyer,†,‡
R. G. Johnson,* and P. B. Hackett, Jr.*,§,[1]

*Department of Genetics and Cell Biology, University of Minnesota, St. Paul, Minnesota 55108-1095; †Department of Pediatrics, and ‡Department of Cell Biology and Physiology, Washington University School of Medicine, St. Louis, Missouri 63110; and §Institute of Human Genetics, University of Minnesota, Minneapolis, Minnesota 55455

Communication via gap junctions provides a mechanism for the cell–cell transfer and coordination of developmental signals. The spatial restriction of gap junctions may also serve to organize cells into domains of coordinated behavior. To investigate the role of gap junctions during embryogenesis, we have characterized the expression of a member of the gap junction gene family, zebrafish *connexin43.4*, a homolog of *connexin45* in chicken and mammals. Expression of *connexin43.4* was induced in the early gastrula, coincident with the first definitive assignments of axial cell fate and the onset of the cell movements comprising convergence and extension in zebrafish. *In situ* hybridization and immunohistochemistry revealed that during gastrulation *connexin43.4* mRNA and protein were progressively enriched in the germ ring and in the notochord primordia on the dorsal side of the embryo. Later in development *connexin43.4* expression was detected in the notochord, the paraxial mesoderm, and the tail bud but was not observed after the differentiation of these tissues. In *no tail* mutant embryos which are defective in tail formation and proper morphogenesis of the notochord, *connexin43.4* expression was absent during gastrulation from the caudal embryonic shield and notochord primordia. During somite stages in *no tail* embryos, *connexin43.4* expression remained absent in the notochordal precursor cells and was lost in the tail bud. Thus, the *no tail* gene product, a transcription factor, was required for the expression of *connexin43.4* in both the notochord and tail bud during morphogenesis. By microinjection of mRNA coding for a connexin43.4/green fluorescent protein fusion in the 1-cell zebrafish embryo, we showed that connexin43.4 is capable of assembling into structures reminiscent of gap junctions. The progressively restricted, developmental expression of the zebrafish *connexin43.4* gene suggests that this gap junctional protein participates in the coordination of gastrulation and the formation of the notochord and tail.

INTRODUCTION

Extensive interactions and coordinated migrations of cells dramatically restructure the blastoderm during gastrulation into three primary germ layers and reveal the embryonic axis. In zebrafish, the cell movements of involution, ingression, and convergent extension have been described during gastrulation and appear to be closely linked to cell specification and axis formation (Kimmel *et al.*, 1990; Warga and Kimmel, 1990; Shih and Fraser, 1995). Critical to the patterning of the embryonic axis is the formation of the dorsal mesoderm and later the notochord, a dorsal mesoderm derivative (Yamada *et al.*, 1991; Halpern *et al.*, 1993; Danos and Yost, 1995). In *Xenopus*, growth factors have been identified which have the ability to induce dorsal mesoderm and *Brachyury* gene expression (reviewed in Moon and Christian, 1992). The zebrafish *no tail* (*ntl*) gene is a homolog of the mouse *T* and *Xenopus Brachyury* genes which encode transcription factors that appear to be important for the formation of both mesoderm and notochord (Schulte-Merker *et al.*, 1992, 1994). Mutations in the zebrafish *ntl* gene and the mouse *T* gene cause a lack of differentiated notochord and posterior structures (Halpern *et al.*, 1993; Schulte-Merker *et al.*, 1994). However, the targets of

[1] To whom correspondence should be addressed. Fax: (612)-625-5754. E-mail: perry@biosci.cbs.umn.edu.

0012-1606/96 $18.00

ntl and *T* proteins are poorly understood but could be involved in cell interactions associated with morphogenetic cell movements and cell adhesion (Wilson *et al.*, 1995).

One mechanism by which cells interact with one another involves the intercellular diffusion via gap junctions of ions and cytoplasmic signals such as inositol phosphates (Saez *et al.*, 1989; Boitano *et al.*, 1992), cAMP (Murray and Fletcher, 1984), and Ca^{2+} (Saez *et al.*, 1989; Charles *et al.*, 1992). Gap junctions are composed of proteins, encoded by a large family of genes called connexins, which form water-filled channels that allow the somewhat nonselective diffusion of molecules up to 1×10^3 M_r between the cytoplasms of adjacent cells (for review see Beyer *et al.*, 1990; Bennett *et al.*, 1991). The formation of gap junctions by the head-to-head alignment and aggregation of these channels in a number of diverse cell types and tissues is believed to allow the coordination of cellular behavior and the response to local signaling (reviewed in Sanderson *et al.*, 1994). In addition, the control of gap junctional communication in the early *Xenopus* embryo appears to be a target of certain members of the *Wnt* and *Activin* classes of signaling molecules which are thought to be involved in axis formation (Olson *et al.*, 1991; Olson and Moon, 1992).

Gap junctional communication and connexin gene expression are organized in a spatially restricted manner during embryogenesis, suggesting that gap junctions allow the cell–cell transfer of developmental signals and coordinate cellular behavior in distinct regions of the embryo (Guthrie, 1984; Martinez *et al.*, 1992; Ruangvoravat and Lo, 1992; Yancey *et al.*, 1992). Programmed differences in cell adhesion provide a model for the driving forces of morphogenetic cell movements. Gap junctional communication may participate in these processes. Evidence in tissue culture cells shows that not only is cell adhesion required for gap junction formation (Mege *et al.*, 1988), but that connexins may also influence the establishment of cell adhesion (Meyer *et al.*, 1992). In further support of this idea, inhibition of gap junctional communication by injection into individual cells of anti-connexin antibodies (Warner *et al.*, 1984; Lee *et al.*, 1987; Fraser *et al.*, 1987), antisense RNA (Bevilacqua *et al.*, 1989), or dominant-negative inhibitor forms of connexins (Paul *et al.*, 1995; Sullivan and Lo, 1995) results in defects in cellular adhesion, cell migration, and patterning in early embryos. In addition, disruption of the *connexin43* gene in mice clearly demonstrates a requirement for gap junctional communication in the development of the heart (Reaume *et al.*, 1995). These observations suggest that gap junctional communication is involved in the control of patterning in the early embryo, possibly by establishing and/or maintaining differences in cell adhesion and permitting the cell–cell transfer of developmental signals.

The analysis of the expression of specific connexins provides important insights into the potential functional roles of gap junctional communication during embryogenesis. For example, the regulation of gap junctions composed of different connexins is dramatically different, and the types of molecules allowed to pass also differ (Laing *et al.*, 1994; Steinberg *et al.*, 1994; Veenstra *et al.*, 1994). Moreover, the expression of one connexin can alter the permeability of gap junctions composed of another connexin, as in the case of *connexin45* (*Cx45*) (Koval *et al.*, 1995). In the present study, we examined the embryonic expression of zebrafish *connexin43.4* (*Cx43.4*), which is closely related to avian and mammalian *Cx45*, in different genetic backgrounds in order to determine its possible roles during development. Our results suggest that *Cx43.4* participates in mediating communication between cells undergoing morphogenetic movements and differentiation and that its expression participates in a developmental pathway for formation of the notochord and tail.

MATERIALS AND METHODS

Zebrafish Stocks and Embryo Collection

Zebrafish were maintained in a constant flow-through water system (Westerfield, 1993). The clonal line C32, provided by Dr. Monte Westerfield, was used in all experiments except where noted. Zebrafish heterozygous for the ntl^{b160} allele were generously provided by Dr. Marnie Halpern. All embryos were obtained from spontaneous spawnings, maintained at 28.5°C, and staged according to Kimmel *et al.* (1993).

cDNA Cloning and DNA Sequencing

The *Cx43.4* cDNA was identified in a low-stringency screen (Sambrook *et al.*, 1989) of a Lambda ZAP II (Stratagene) cDNA library prepared from somite stage (9 to 16 hr) zebrafish embryo mRNA. After plaque purification, plasmids were excised *in vivo* from phage clones, and the *Cx43.4* cDNA clone was sequenced by the dideoxy chain-termination method (United States Biochemical). Nucleic acid and protein sequence analyses were carried out using Intellegenetics and the Genetics Computer Group software packages, respectively.

RNA Analysis

Total RNA was extracted from staged zebrafish embryos (Puissant and Houdebine, 1990). Groups of 100 embryos were homogenized by five passages through a 19-gauge needle in 0.45 ml of solution D (4 *M* guanidinium thiocyanate, 25 m*M* sodium citrate, pH 7.0, 0.5% sodium sarcosyl, 0.1 *M* 2-mercaptoethanol). After isolation, 10 μg of total RNA was loaded in each lane for electrophoresis through a formaldehyde–1% agarose gel and blotted to Nytran membrane (Schleicher & Schuell); equal loading of RNA in each lane was verified by visualization of rRNA by ethidium bromide staining before transfer. Northern hybridizations were carried out in 50% formamide, 5× SSPE, 5× Denhardt's solution, 1% SDS, 100 μg/ml yeast RNA (Sigma) at 60°C with RNA probes produced by *in vitro* transcription (Ambion) in the presence of [α-^{32}P]ATP (Amersham). A *Cx43.4* probe complementary to *Cx43.4* mRNA was produced from the same template as described below for *in situ* hybridizations. An RNA probe transcribed from the zebrafish *eF-1α* gene, kindly provided by Dr. Walter Sauerbier, was used to verify the integrity of the RNA in each sample. Membranes were washed at high stringency in 0.1× SSPE, 0.1% SDS at 65°C.

Anti-connexin Antibodies

Rabbit polyclonal antisera directed against a synthetic peptide representing amino acids 285–298 (SAPPGYNIAVKPDQ) of canine Cx45 were described previously (Kanter *et al.*, 1992). The anti-Cx45 antibodies were affinity-purified by chromatography using a Sulfolink–agarose coupling gel (Pierce Chemical Co.) derivatized with the specific immunogenic peptide according to manufacturer's instructions and eluted with 0.1 *M* glycine at pH 3.0. We have previously demonstrated the specificity of these antibodies for *in vitro* translated connexins by immunoprecipitation and by immunofluorescence microscopy (Kanter *et al.*, 1993).

Immunoprecipitation and Western Blots

Constructs of the *Cx43.4* used for *in vitro* translation were the full-length cDNA, and a cDNA truncated in the 3′ end at nucleotide position 934 (*Cx43.4*Δ*ct*) and fused in frame to the green fluorescence protein (GFP) gene (Prasher *et al.*, 1992). mRNA was transcribed in the presence of 6 m*M* cap analog (^{7m}GpppG) using the Megascript kit (Ambion) and translated *in vitro* with rabbit reticulocyte lysates (Promega). Embryos were staged and frozen in a minimal amount of PBS at −80°C until use. After homogenization and sonication, samples were incubated overnight with constant rotation in 1 ml of RIPA buffer (PBS containing 1% Triton X-100, 0.6% SDS, 1000 U/ml aprotinin, 0.1% pefabloc, 1 m*M* sodium orthovanadate, and 1 m*M* sodium fluoride). Samples were microfuged for 30 min, and the supernatants were collected. The connexin protein was immunoprecipitated with 1 μg of the anti-Cx45 antibodies and 20 μl of protein A Sepharose fast flow (Pharmacia) as outlined in Laing *et al.* (1994) and Darrow *et al.* (1995). After 2 hr of rotation at 4°C, tubes were briefly centrifuged, and the immunoprecipitated material was collected and washed four times for 15 min each in 1 ml of RIPA buffer. The immunoprecipitated material was analyzed by SDS–PAGE and transferred to Immobilon-P (Millipore) as in Laing *et al.* (1994). The membrane was blocked with PBS containing 1% Triton X-100, 1% gelatin, and 1 mg/ml anti-rabbit IgG and incubated with the anti-Cx45 antibody at a 1:200 dilution (Laing *et al.*, 1994) in PBS containing 0.5% Triton X-100 (PBSTX). The membrane was washed four times for 15 min each in PBSTX, incubated in a horseradish peroxidase-conjugated anti-rabbit IgG (Hyclone) at a 1:2000 dilution in PBSTX, and developed with the ECL chemiluminescence detection system (Amersham).

Whole-Mount in Situ Hybridization and Immunohistochemistry

Whole-mount *in situ* hybridizations were performed by the method of Schulte-Merker *et al.* (1992). Permeabilization of embryos with Proteinase K was limited to 5 min, and hybridizations were carried out at 65 to 70°C. After detection, embryos were cleared in benzyl benzoate:benzyl alcohol (2:1) and observed and photographed using DIC optics on a Leitz microscope. For thick sectioning after hybridization and detection, embryos were dehydrated stepwise through an ethanol series and placed in 1:1 ethanol:Quetol 651 (Ted Pella, Inc.) with gentle mixing for 30 min. Embryos were then infiltrated with Quetol 651 for at least 1.5 hr and polymerized overnight at 72°C. Ten-micrometer sections were cut using a glass knife and mounted in Permount.

Sense and antisense digoxigenin-labeled RNA probes were prepared by *in vitro* transcription from linearized templates of *Cx43.4* cDNA clone in the pBlueScript vector (Stratagene). Either the T3 or T7 promoter was used for transcription in the presence of digoxigenenin-11–UTP (Boehringer-Mannheim) using a Maxiscript kit (Ambion). No hybridization signal was detected in control hybridizations using a sense RNA probe produced from the *Cx43.4* cDNA (data not shown).

Whole-mount immunohistochemistry was performed using the method of Halpern *et al.* (1993). After fixation overnight at 4°C in 4% paraformaldehyde in PBS and washing in PBST (PBS with 0.1% Tween 20), embryos were permeabilized in acetone for 7 min at −20°C, washed in PBST, and blocked for 1 hr at room temperature in 5% goat serum, 1% bovine serum albumin, 1% dimethyl sulfoxide (DMSO) in PBST. Embryos were incubated overnight at 4°C with the affinity-purified, anti-Cx45 antibodies (Kanter *et al.*, 1992) diluted 1:1000 in the blocking solution. Embryos were washed eight times in 1% bovine serum albumin, 1% DMSO in PBST. A secondary goat anti-rabbit FITC-conjugated polyclonal antibody (Boehringer-Mannheim) was absorbed at a 1:500 dilution to embryos and washed as before. Embryos were dissected away from the yolk, cleared in 50% glycerol/PBST solution, and mounted in the same solution with 1 mg/ml *p*-phenylenediamine. Embryos were examined using either a Leitz microscope with epifluorescence illumination or a Nikon diaphot microscope with an MRC-600 confocal imaging system (Bio-Rad Labs) using a 60 X/1.4 planapochromat lens.

Cx43.4/GFP mRNA and Microinjection

The zebrafish *Cx43.4* coding sequence was PCR amplified from the full *Cx43.4* cDNA using Vent polymerase (New England Biolabs) to remove the termination codon and add a *Nhe*I restriction endonuclease site with the following oligonucleotides: (5′-GAG GAA AAG AGT GGA AAT C-3′) and (5′-TCA AGC TAG CAT GGA TCC CTT TTT CAC A-3′). The *Cx43.4* PCR product was digested with *Nhe*I and ligated in frame with the coding sequence of the GFP (Crameri *et al.*, 1995) digested with *Nhe*I and *Eco*RI. The *Xenopus* β-globin 3′UTR (untranslated region) was added to increase the stability and translation of the synthetic mRNA after microinjection. Synthetic RNA was transcribed from the T7 promoter of the *Cx43.4*/GFP fusion gene in pBlueScript as above. The mRNA was purified by phenol:chloroform extraction (1:1), precipitated, and resuspended in RNase-free water. The concentration of the synthetic RNA was adjusted to 0.5 μg/μl, and rhodamine-dextran (Molecular Probes) was added to 0.1% before microinjection into zebrafish embryos at the 1-cell stage. Confocal microscopy images of living embryos were taken using a 20X planapochromat lens as above.

RESULTS

Isolation and Characterization of the Zebrafish connexin43.4 cDNA

From a low-stringency screen of a cDNA library made from zebrafish embryos at the segmentation period of development, we isolated a 2.2-kb cDNA that contains an open reading frame encoding a polypeptide of 380 amino acids with a predicted molecular mass of 43.4 kDa (Fig. 1). The open reading frame is flanked by a 5′UTR of 85 nucleotides and a 3′UTR of 1008 nucleotides con-

FIG. 1. Nucleotide and predicted amino acid sequence of *Cx43.4.* The poly(A) signal (nucleotides 2214–2218) is underlined. GenBank Accession No. L46801.

nected to a poly(A) tail. Hydropathy analysis (Kyte and Doolittle, 1982) of the predicted polypeptide suggests four hydrophobic, transmembrane domains within this protein similar to connexins from other vertebrate species (boxed regions in Fig. 2A). The amino acid sequence also contains conserved cysteines in the putative external loop domains at positions 53, 60, 64, 212, 217, and 223, which are indicative of connexin structure (Fig. 2). Based on the significant regions of identity to connexins from other vertebrate species and the predicted molecular mass, this cDNA clone was named zebrafish *connexin43.4* (*Cx43.4*).

The amino acid sequence of Cx43.4 is most similar to Cx45 from chickens, mice, dogs, and humans (Fig. 2A). If conservative amino acid substitutions are considered, the zebrafish Cx43.4 has a similarity of 73% to chicken Cx45 and 71–72% to murine, canine, and human Cx45. The zebrafish Cx43.4 has an overall amino acid identity of 57% to chicken and 54% to mouse, dog, and human Cx45. In contrast, the zebrafish Cx43.4 has only a 62% similarity and a 35% identity to the another related connexin, rat Cx43. The similarity of the zebrafish Cx43.4 to Cx45 from other vertebrate species is highest in the predicted transmembrane regions (81–95%) and external loop domains (residues 40–75 and 202–232; 100 and 87%, respectively) of Cx43.4 (Fig. 2A). Hydropathy plots of connexin structures predict a strong structural similarity between the zebrafish Cx43.4 and the mouse Cx45 (Fig. 2B). Although the amino acid similarity of the zebrafish Cx43.4 to the Cx45 from other vertebrates is less in the putative cytoplasmic loop domain between transmembrane regions two and three (residues 97–180; 62–66%) and in the cytoplasmic tail (residues 247–380; 52–56%), hydropathy plots for Cx43.4 and mouse Cx45 suggest a conservation of overall structure and, therefore, function.

Temporal Expression of Cx43.4

Northern blot analysis of RNA isolated from different developmental stages identified a single band of approximately 2.3 kb which hybridized with a probe prepared from the *Cx43.4* cDNA, suggesting that there is one predominant species of *Cx43.4* mRNA and that the cloned 2.25-kb cDNA is nearly full-length (Fig. 3A). *Cx43.4* was expressed during oogenesis, although only very limited levels of *Cx43.4* mRNA were found in the 1-cell zebrafish embryo. A low level of *Cx43.4* mRNA was detected throughout the blastula stages. *Cx43.4* expression was sharply induced between 50% epiboly and the

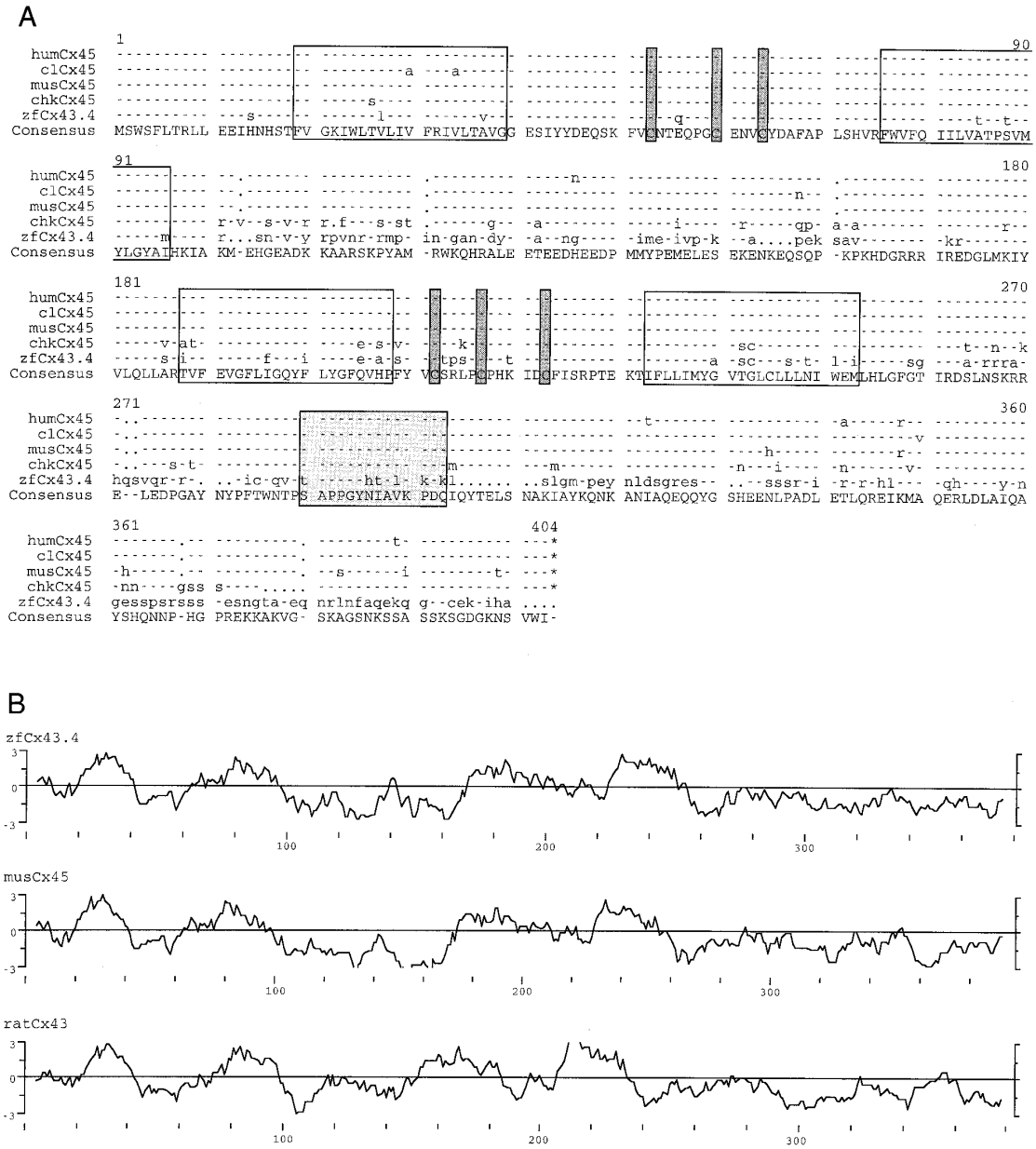

FIG. 2. (A) A comparison of the similarity of the zebrafish Cx43.4 (zfCx43.4) to chicken (chkCx45; Beyer, 1990), mouse (musCx45; Hennemann *et al.*, 1992), canine (clCx45; Kanter *et al.*, 1992), and human (humCx45; Kanter, *et al.*, 1994) Cx45 polypeptides. The predicted transmembrane domains are boxed. Conserved cysteine residues are boxed in dark gray, and the synthetic peptide used for generation of the anti-Cx45 antibodies (Kanter *et al.*, 1992) is boxed in light gray (residues 289–303). (B) Kyte-Doolittle hydrophobicity plots of the zebrafish Cx43.4, and the mouse Cx45 and rat Cx43 (Beyer *et al.*, 1987) polypeptides.

shield stage of gastrulation (Fig. 3A; and data not shown). Expression was maintained at high levels throughout gastrulation and the early somite periods of development. The level of *Cx43.4* mRNA declined during later somite stages, with low levels detected during pharyngula and hatching periods of development. By Day 5 of development, *Cx43.4* mRNA was not detectable by Northern blot analysis.

To examine whether the relative abundance of the Cx43.4 polypeptide correlates with the accumulation of *Cx43.4* mRNA during embryogenesis, affinity-purified anti-Cx45 antibodies, raised to a synthetic peptide representing amino acid residues 285–298 (Fig. 2A; light gray box) of the canine Cx45 (Kanter *et al.*, 1992), were used in immunoprecipitation and immunoblotting experiments.

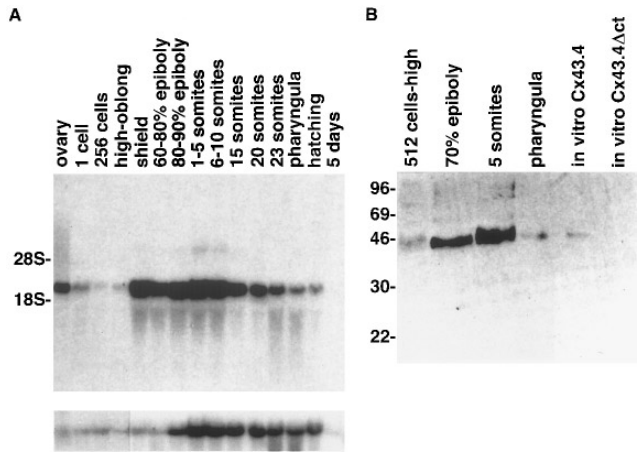

FIG. 3. Temporal expression of *Cx43.4*. (A) Upper panel: Northern blot hybridized with an antisense *Cx43.4* RNA probe. 10 μg of total RNA was loaded in each lane for each developmental stage indicated. The mobilities of the 18S (2.1 kb) and the 28S (5.2 kb) rRNAs are indicated at the side. Lower panel: The same membrane was rehybridized with an antisense eF-1α RNA probe as a control for integrity of the mRNA. (B) Western blot of immunoprecipitated Cx43.4 protein from embryos. The first four lanes represent 10 embryos from each stage. The lanes labeled *in vitro* Cx43.4 and Cx43.4Δct involve immunoprecipitations of proteins translated *in vitro* from *Cx43.4* mRNA and a mutant *Cx43.4* mRNA lacking most of the anti-Cx45 epitope region, respectively.

This region is exactly conserved in all of the mammalian and avian Cx45 sequences and 8 of 14 residues are identical in the zebrafish Cx43.4. Immunoprecipitated proteins from different developmental stages of zebrafish embryos were analyzed by SDS–PAGE and Western blotting with the anti-Cx45 antibodies. As shown in Fig. 3B, the antibody detected a polypeptide of approximately 43 kDa, which matches the molecular mass predicted from the amino acid sequence of zebrafish Cx43.4. A lower level of the Cx43.4 polypeptide was detected in extracts from the midblastula (Fig. 3B, designated 256 cells and high-oblong) and pharyngula (Fig. 3B, pharyngula) stages than from gastrula (Fig. 3B, 70% epiboly) and somite (Fig. 3B, 5 somites) stages. The relative abundance of the Cx43.4 polypeptide correlated with the level of *Cx43.4* mRNA during these stages of development. As a control for antibody specificity, proteins were translated *in vitro* in a rabbit reticulocyte lysate programmed with either *Cx43.4* mRNA or *Cx43.4* mRNA lacking most of the carboxyl terminus (Cx43.4Δct, amino acids 1 to 283) and analyzed in the same manner (Fig. 3B). A polypeptide of 43 kDa was detected in both the embryo extracts and the *in vitro* extract programmed with *Cx43.4* mRNA. This band was not observed with the translation products from the truncated *Cx43.4* mRNA, which lacks most of the region used for antibody generation.

Spatial Expression of Cx43.4 during Development

Theoretically, intercellular communication within domains of the developing embryo is mediated by specific connexins. To determine the possible roles of *Cx43.4* during embryonic development, we determined where *Cx43.4* is expressed using whole-mount *in situ* hybridization with digoxigenin-labeled RNA probes. An antisense probe complementary to the *Cx43.4* mRNA was produced from the cytoplasmic tail region and 3′UTR of the *Cx43.4* cDNA. This probe, which lacks the transmembrane regions of the *Cx43.4* cDNA, was used in order to avoid possible cross-reactivity with other connexins which may be expressed during similar stages of development. However, a full-length probe produced similar results. As shown in Fig. 4A, expression of *Cx43.4* was detected during the primary growth phase (stages Ia/Ib) of early oogenesis, as defined by Selman *et al.* (1993). Consistent with low levels of *Cx43.4* mRNA detected in the early embryo by Northern analysis (Fig. 3A), expression was not observed at later stages of oogenesis by *in situ* hybridization. During blastula stages low levels of *Cx43.4* mRNA were observed ubiquitiously throughout the blastomeres of the embryo but not within the yolk cell (Fig. 4B).

At the beginning of gastrulation in zebrafish, ingression of cells at the blastoderm margin produces two layers of cells, the primary-ectoderm and the primitive-hypoblast, and a local thickening around the circumference of the embryo called the germ ring (Warga and Kimmel, 1990; Shih and Fraser, 1995). As gastrulation proceeds the cell movements of convergence and extension produce an additional thickening in the germ ring, the embryonic shield, which defines the dorsal side of the embryo. Expression of *Cx43.4* was induced during the formation of the embryonic shield and became spatially enriched in both the germ ring and embryonic shield (Figs. 4C and 4D). The enrichment of *Cx43.4* expression in the germ ring and on the dorsal side of the embryo persisted through later gastrula stages as shown at 85% epiboly (Figs. 4E and 4F). Sectioning of gastrula stage embryos after whole-mount *in situ* hybridization showed *Cx43.4* mRNA in both the primary-ectoderm and primitive-hypoblast of the germ ring (Fig. 4G). Sectioning also verified the enrichment of *Cx43.4* mRNA in both the germ ring and the dorsal side of the embryo (data not shown). However, there was no expression of *Cx43.4* in the most posterior region of the embryonic shield and in the overlying primary-ectoderm at late gastrula stages, which may affect the ability of these cells to communicate with surrounding cells (arrows in Figs. 4E, 4F, and 4H).

After blastopore closure, which marks the end of gastrulation, cells continue to converge and extend along the dorsal midline causing the embryo to lengthen along its anterior–posterior axis. During the early segmentation periods of development, *Cx43.4* mRNA was found enriched in the notochord, paraxial hypoblast, and tail bud (Figs. 5A, 5B, and 5C). Expression in the cells which form the notochord was initiated during gastrulation (see below) and persisted

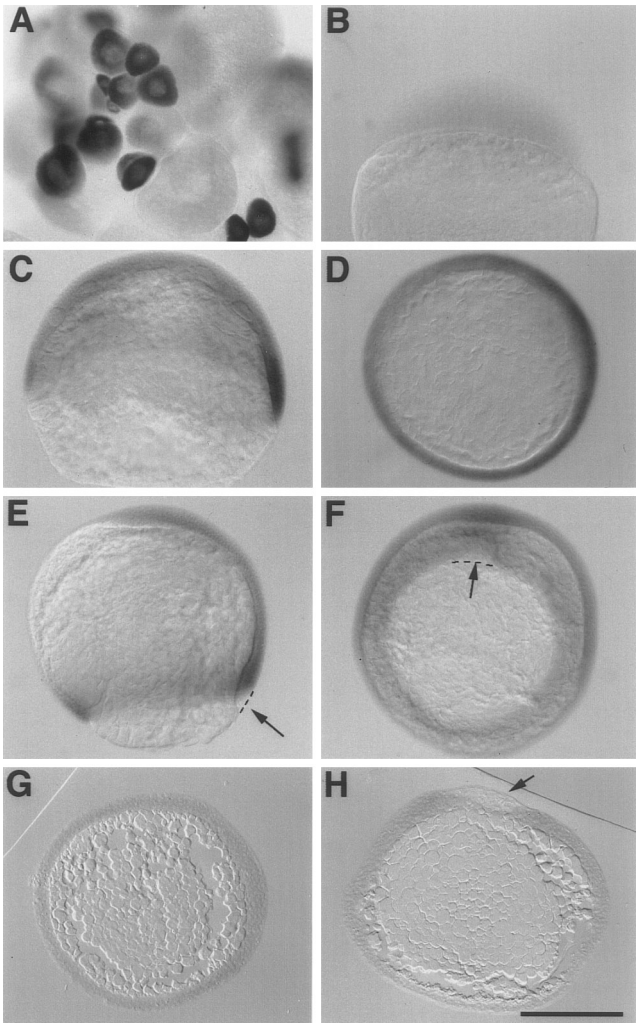

FIG. 4. Whole-mount *in situ* hybridization of *Cx43.4* mRNA during oogenesis and gastrulation. (A) Ovary. (B) 1-K cell stage, side view. (C and D) Shield stage, side and vegetal pole views, respectively; dorsal is to the right for both embryos. (E) 85% epiboly; side view with dorsal to the right. (F) 85% epiboly, vegetal pole view with dorsal to the top. (G) Section through the germ ring of an 85% epiboly embryo, dorsal to the right. Dashed lines mark the blastoderm margin in E and F. (H) Section through the germ ring of a 70% epiboly embryo in a more caudal position than in (G); dorsal is to the top. Arrows in E, F, and H point to unlabeled cells in the caudal embryonic shield. The magnification is the same for all panels; scale bar in H, 250 μm.

through early somite stages during notochord formation (Figs. 5B and 5C; large arrows). By the 10-somite stage, expression of *Cx43.4* was greatly reduced in the notochord (Fig. 5D). Expression in the paraxial hypoblast occurred only transiently and was absent by the time somites were formed (Figs. 5A, 5B, 5C, and 5D; small arrows). *Cx43.4* expression was found in the tail bud (Figs. 5A, 5B, 5C, and 5D; large arrows in A). Sectioning of embryos after whole-mount *in situ* hybridization verified the expression of *Cx43.4* within the notochord (Fig. 5E; arrow), paraxial hypoblast (Fig. 5F; arrow), and tail bud (Fig. 5E).

During the 17- to 20-somite stages, *Cx43.4* expression persisted in the tail bud and increased in the anterior central nervous system (CNS) within the developing eyes, midbrain, and hindbrain (Figs. 6A and 6B). At the end of the segmentation period, the domain of *Cx43.4* expression became limited to the most posterior region of the tail where the last somites are formed (Fig. 6C). When the extension of the tail was complete, expression of *Cx43.4* in this region of the embryo was lost (data not shown). By the end of the segmentation period, *Cx43.4* expression in the midbrain became restricted to ventral regions (Figs. 6C and 6D). By the early pharyngula period, expression within the hindbrain became restricted to the floor plate of the CNS (Figs. 6E and 6F; arrows) and to groups of cells lateral to the floor plate which appeared to correspond to ventral rhombomere centers.

To ensure that the spatial distribution of Cx43.4 protein paralleled that of the *Cx43.4* mRNA *in situ*, whole-mount immunohistochemical staining using affinity-purified, anti-Cx45 antibodies (Kanter *et al.*, 1992) was performed on staged zebrafish embryos. As shown in Fig. 7A, a punctate pattern of staining was observed within the germ ring in mid-gastrula stage embryos (arrow marks the margin of the blastoderm), similar to the appearance of immunohistochemical staining for gap junctions in tissue culture cells and mouse embryos (Laing *et al.*, 1994; Yancey *et al.*, 1992). This punctate pattern of staining was not observed when the primary antibody was omitted or a different primary antibody was used with the same secondary antibody (data not shown). The punctate pattern was also detected in cells located around the site of blastopore closure at the end of gastrulation (Fig. 7B; arrow) and in the notochord at the 2-somite stage (Fig. 7C; arrow). Optical sectioning of the embryos using scanning confocal microscopy revealed that the punctate staining pattern appeared to be associated with cellular boundaries (Fig. 7D).

To further show that Cx43.4 is capable of assembling into structures reminiscent of gap junction plaques, we injected zebrafish embryos with synthetic mRNA made from a fusion between the complete *Cx43.4* coding sequence and GFP. Using scanning confocal laser microscopy, the Cx43.4/GFP fusion protein was imaged in living embryos at the late blastula period and appeared as punctate and elongated spots in the embryo (Fig. 7E). Expression of the GFP alone was observed throughout the blastomeres (data not shown), suggesting that the localization of the Cx43.4/GFP fusion protein to the intensely fluorescing plaques was due to sequences contained within the Cx43.4 protein. To visualize the blastomeres, the *Cx43.4*/GFP mRNA was co-injected with rhodamine-labeled dextran. Superimposing images from the expression of the *Cx43.4*/GFP mRNA and the rhodamine-dextran showed that many of the punctate spots localized to regions of cell apposition, as expected for a connexin protein. Optical sectioning of the embryo sug-

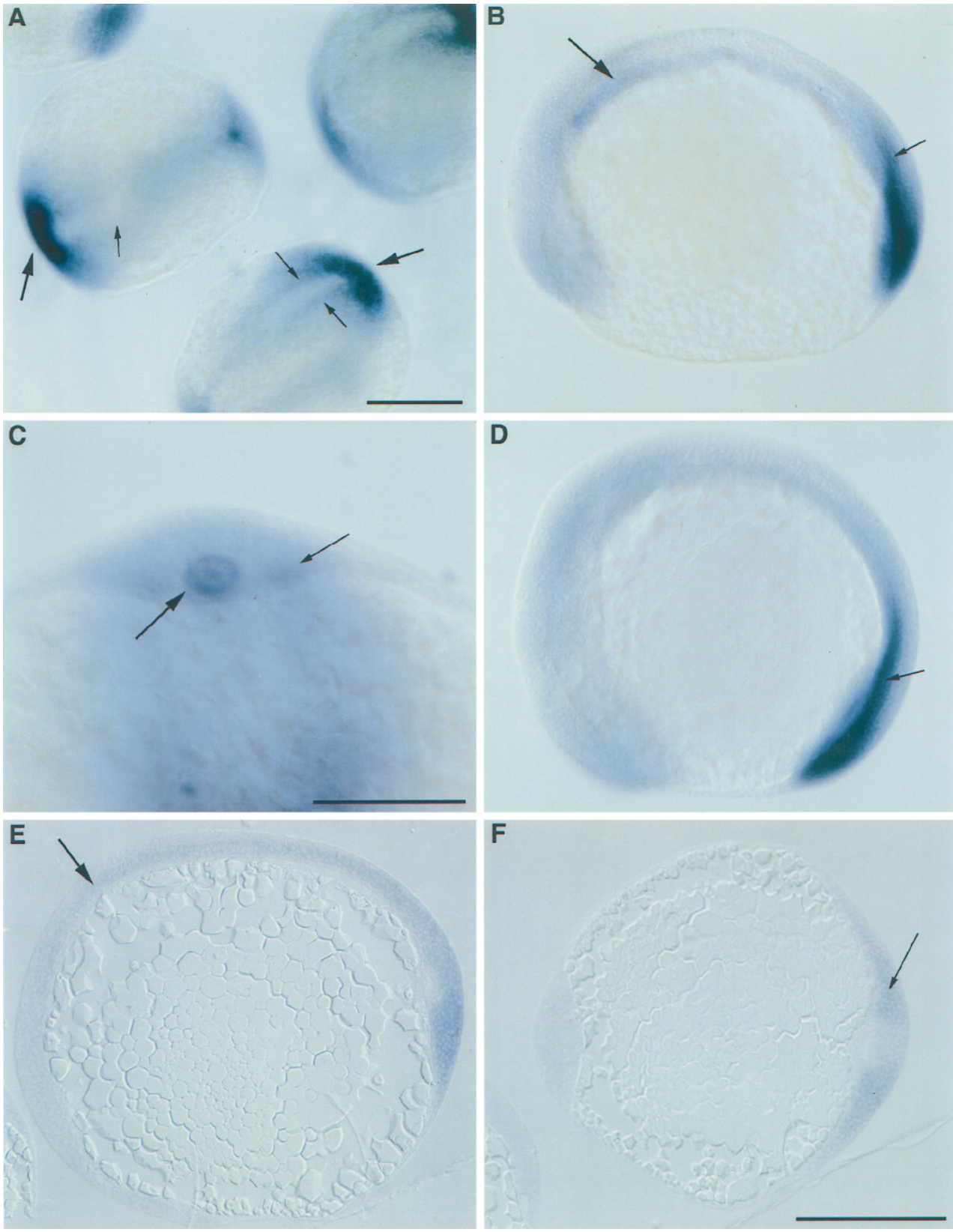

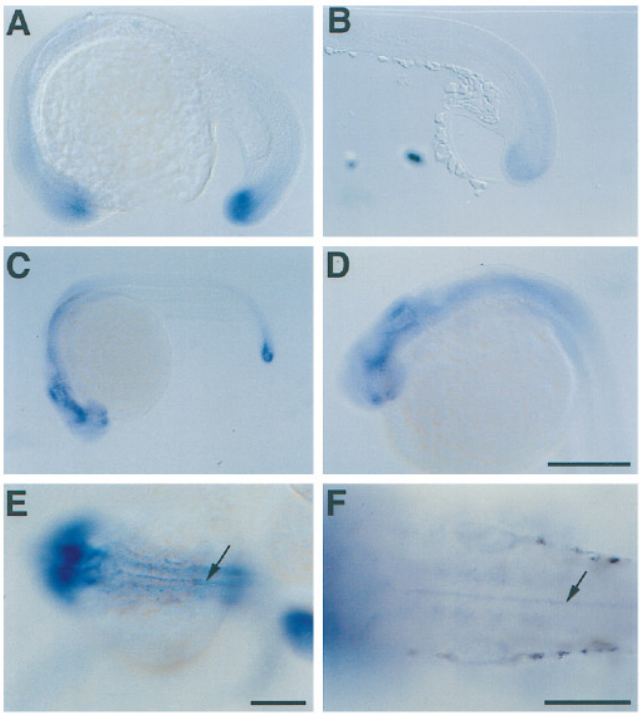

FIG. 6. Whole-mount *in situ* hybridization of *Cx43.4* mRNA during late segmentation and pharyngula periods. (A) 20-somite stage embryo; side view with anterior to the left. (B) Sagital section through the tail at the 17-somite stage. (C and D) End of segmentation period; side view with anterior to the left. (E and F) Pharyngula period (30 hr); dorsal view with anterior to the left. Arrows point to the floor plate of the central nervous system. Scale bars: D, 250 μm, and the magnification is the same for A and B; E, 250 μm, and the same for C; F, 100 μm.

gested that some of the observed fluorescence was between cells in different focal planes. Certain other sources of fluorescence that do not correspond to regions of cell apposition could represent the fusion protein at intracellular sites or at the cell surface in the process of assembling into gap junctions. We have also observed rings of fluorescence with the Cx43.4/GFP fusion protein and interpret these structures as the incorporation of the fusion protein at the periphery of preexisting gap junctions.

Expression of Cx43.4 in no tail Mutant Embryos

The observations that *Cx43.4* was expressed in the notochord and tail bud suggested that *Cx43.4* gene expression participates in a pathway for notochord and tail formation. To further explore this possibility and understand how *Cx43.4* expression is controlled, we examined *Cx43.4* expression in *ntl* mutant zebrafish embryos which show defects in the proper differentiation of the notochord and formation of the tail (Halpern *et al.*, 1993). At 90% epiboly in wild-type embryos, *Cx43.4* mRNA was detected within the notochord primordia (Fig. 8A; large arrow) and within the caudal embryonic shield (Fig. 8A; small arrow). In contrast, in *ntl* mutant embryos *Cx43.4* expression was absent from the notochordal precursor cells (Fig. 8C; large arrow) and from the caudal embryonic shield (Fig. 8C; small arrow). At the tail bud stage in wild-type embryos, *Cx43.4* was expressed in the differentiating notochord (Fig. 8B; arrow), paraxial mesoderm, and tail bud. However, at the tail bud stage in the *ntl* mutant embryos, *Cx43.4* mRNA was not present in the notochordal precursor cells (Fig. 8D; arrow) and was absent from more axial cells in the paraxial hypoblast and tail bud. Later in development in wild-type embryos, *Cx43.4* was expressed in the tail bud until formation of the tail was complete at the beginning of the pharyngula period. In contrast, in *ntl* mutant embryos which have defects in tail extension, *Cx43.4* mRNA was absent within the tail bud by late segmentation (data not shown).

DISCUSSION

The zebrafish *Cx43.4* cDNA predicts a polypeptide containing four putative membrane-spanning domains and a number of conserved cysteine residues, similar to connexins from other vertebrates. Based on structural comparison, the similarity of hydropathy plots, and the recognition of the *in vitro* translated Cx43.4 polypeptide by the anti-canine Cx45 antibodies, we conclude that *Cx43.4* from zebrafish is a homolog of *Cx45* from other vertebrates. The pattern of Cx43.4 localization in zebrafish embryos coincided with the distribution of *Cx43.4* mRNA and suggests that the Cx43.4 polypeptide is assembled into gap junctions. This hypothesis is strengthened by the observation that the Cx43.4/GFP fusion protein localizes to regions of cell apposition, indicating that the fusion protein is capable of assembling into fluorescent plaques resembling gap junctions.

Expression of Cx43.4 during Embryogenesis

Gap junctions formed from mammalian Cx45 are unusual in that they do not allow efficient transfer of the dye Lucifer

FIG. 5. Whole-mount *in situ* hybridization of *Cx43.4* mRNA during segmentation. (A) 2- to 5-somite stage; dorsal views. Large arrow, tail bud; small arrows, paraxial mesoderm. Scale bar, 250 μm. (B) 2-somite stage; side view. Large arrow, notochord; small arrow, paraxial mesoderm. (C) 5-somite stage; posterior, transverse view at higher magnification. Large arrow, notochord; small arrow, paraxial mesoderm. Scale bar, 100 μm. (D) 10-somite stage, side view, anterior to the left; arrow points to paraxial tissue. (E) Sagital section of a 1-somite embryo; arrow marks notochord. (F) Transverse section of a 2-somite stage embryo, arrow marks expression in paraxial tissue in the tail. Scale bar in F represents 250 μm and is the same for B, D, and E.

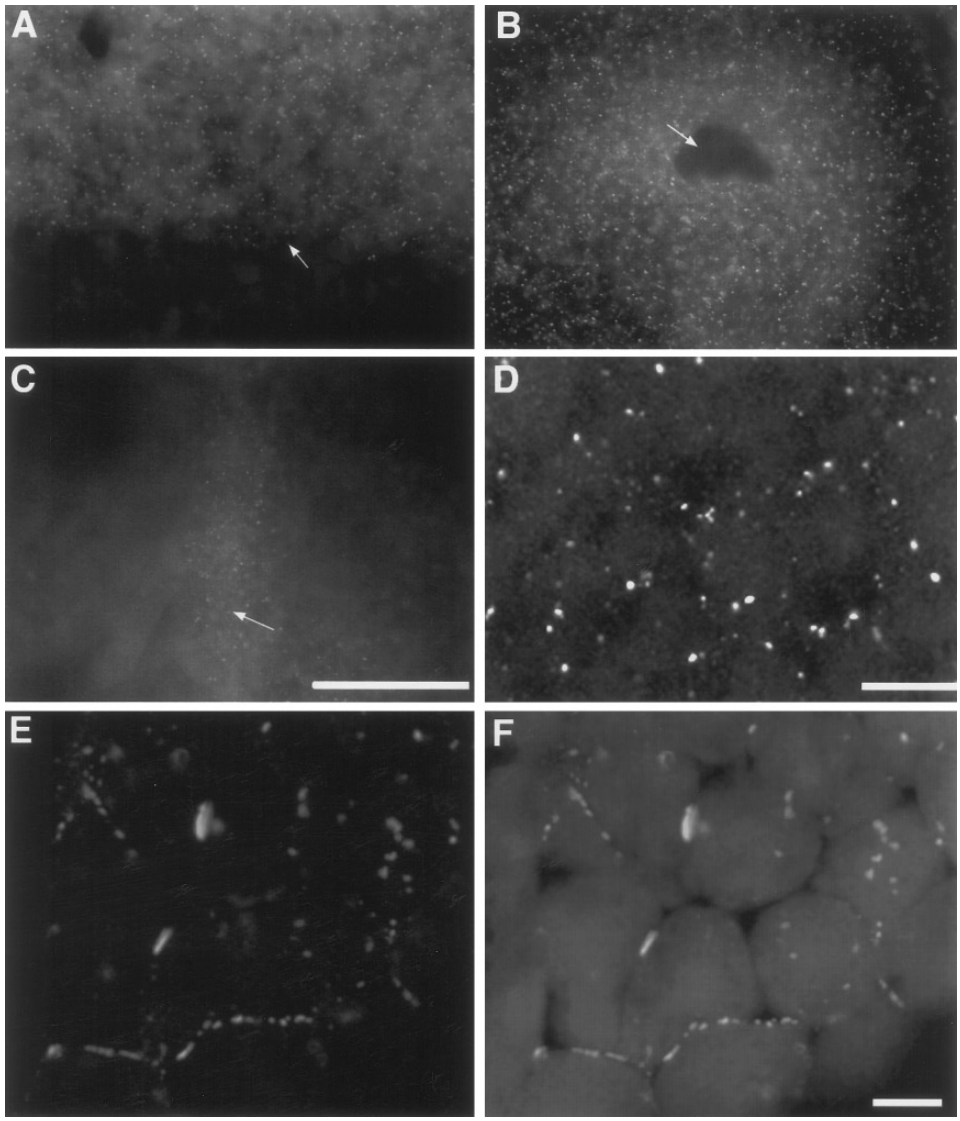

FIG. 7. Cx43.4 protein and *Cx43.4* message are localized during gastrulation and early somite stages to similar regions, and the expression of a Cx43.4/GFP fusion protein during blastula stages localizes to regions of cell apposition. (A–D) Immunohistochemical localization of Cx43.4 protein. (A) Tissue from the germ ring of a shield stage embryo; side view with animal pole toward the top; arrow points to blastoderm margin. (B) Tissue from tail bud of a 1-somite stage embryo; dorsal view with posterior to the top; arrow points to blastopore. (C) Tissue from the trunk region of a 1-somite stage embryo; dorsal view with posterior to the bottom; arrow points to the notochord. (D) Scanning confocal microscopy image of the germ ring of a 70% epiboly stage embryo, side view. (E, F) Confocal microscopy images of a living zebrafish embryo after co-injection of Cx43.4/GFP mRNA and rhodamine-dextran at the 1-cell stage. (E) The Cx43.4/GFP fusion protein was visualized during the late blastula period as an extensive array of fluorescent plaques. (F) Superimposed images of the Cx43.4/GFP protein in E and rhodamine-dextran, showing that most of the fluorescence from the fusion protein is associated with cell surfaces. Scale bar in C represents 100 μm and is the same for A and B; the scale bar in D represents 12 μm and in F, 20 μm.

Yellow between cells, but do permit electrical coupling and the transfer of other dyes such as 2′,7′-dichlorofluorescein (Steinberg *et al.*, 1994; Veenstra *et al.*, 1994). In addition, when Cx45 was transfected into cells expressing endogenous Cx43 and displaying dye transfer, the spread of Lucifer Yellow was suppressed (Koval *et al.*, 1995). Thus, the expression of *Cx43.4* in the zebrafish embryo may also serve to establish restricted communication between specific cells during gastrulation. At the beginning of gastrulation in zebrafish, *Fundulus heteroclitus*, and *Barbus conchonius* embryos, gap junctional communication, as assessed by Lucifer Yellow dye transfer, is lost between the yolk syncitial layer

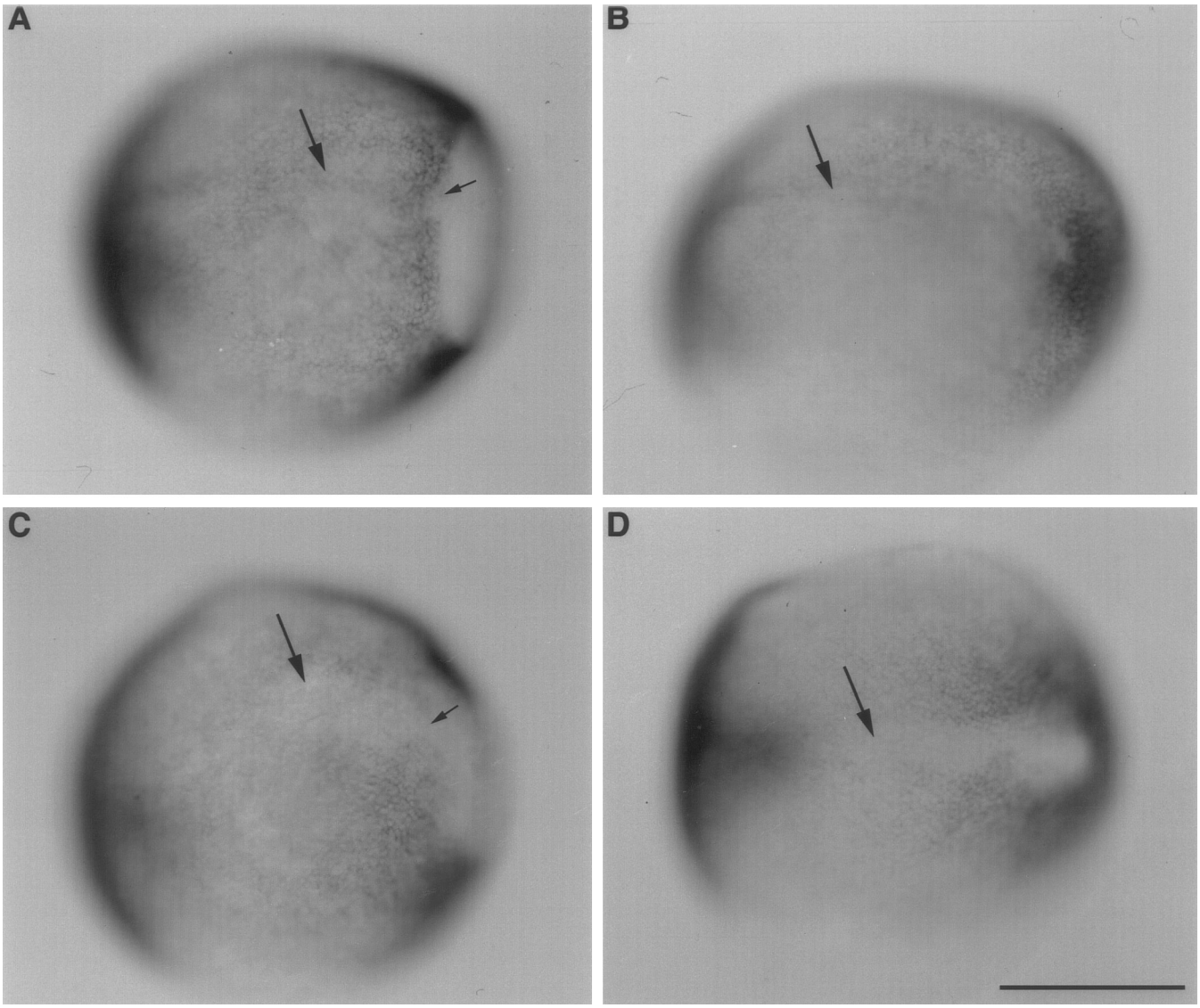

FIG. 8. Whole-mount *in situ* detection of *Cx43.4* mRNA during late gastrulation and tail bud stages in wild-type and *ntl* mutant embryos. (A and B) Wild-type embryos at 90% and tail bud stage, respectively. (C and D) *ntl* mutant embryos at the same two stages, respectively. Dorsal views with animal pole or anterior to the left in all panels. Large arrows point to axial hypoblast showing labeled cells in wild-type embryos and an absence of *Cx43.4* mRNA detection in *ntl* embryos, and small arrows in A and C mark the caudal embryonic shield. Scale bar in D represents 250 μm and is the same for the other panels.

and the blastoderm, while the blastomeres remain in communication with one another (Kimmel *et al.*, 1984; Kimmel and Law, 1985; Gevers and Timmermans, 1991). If the zebrafish Cx43.4 shares permeability properties with Cx45, then the induced expression of *Cx43.4* at the beginning of gastrulation may participate in the observed developmental uncoupling of the yolk syncitial layer from the blastoderm and thereby limit the types of signals which could be transferred from the yolk syncitial layer to the blastoderm.

The induced expression of *Cx43.4* is coincident with the first definitive assignments of axial cell fate and the beginning of the morphogenetic cell movements identified as convergence and extension (Kimmel *et al.*, 1990; Warga and Kimmel, 1990). This result is consistent with the observation of gap junctional communication among blastomeres after the onset of gastrulation (Kimmel and Law, 1985). Later, *Cx43.4* is expressed during gastrulation and tail formation in cells which display common cellular behavior in terms of cell migration and differentiation within the zebrafish embryo. Examples of this include *Cx43.4* expres-

sion in the germ ring in both the primary-ectoderm and primitive-hypoblast, the dorsal side of the embryo as gastrulation proceeded, and later in the paraxial hypoblast and tail bud. Expression of Cx43.4 was lost in cells in these regions after their differentiation. *Cx43.4* shares partially overlapping domains of expression during these periods with the *ntl* gene product and the *snail* gene product, a nuclear, zinc-finger protein thought to be important for proper cell migration (Schulte-Merker *et al.,* 1992; Thisse *et al.,* 1993; Hammerschmidt and Nusslein-Volhard, 1993). The apparent coordinated expression of *ntl, snail,* and *Cx43.4* suggests similar mechanisms for the control of their expression. The induced expression at the beginning of gastrulation and the localization of *Cx43.4* mRNA supports the hypothesis that cells undergoing morphogenetic movements and differentiation are communicating via Cx43.4 gap junctions to coordinate these events.

The tail bud contains populations of cells which have the ability to direct tail formation and give rise to the primary tissue types found within the tail, including the neural tube, notochord, and somites. Observations in *Xenopus* have led to the suggestion that tail formation is a direct continuation of gastrulation within the tail bud, where the dorsal mesoderm retains the ability to induce cell fates and cell movements (Gont *et al.,* 1993). Expression of *Cx43.4* during gastrulation and within the tail bud until tail formation is complete supports this hypothesis. In *ntl* mutant embryos, the absence of *Cx43.4* mRNA by late gastrulation within the embryonic shield and later in a subset of more axial cells in the tail bud correlates with the inability of this region of the embryo to form the tail later in development. The loss of *Cx43.4* expression from the tail of *ntl* mutant embryos most likely reflects an earlier arrest in tail formation. Thus, *Cx43.4* might have a similar function during gastrulation and tail formation that acts downstream of the *ntl* gene product.

A key observation in this study was that *Cx43.4* expression was enriched in the notochord primordia and persisted in the notochord during its early formation, suggesting that *Cx43.4* expression and gap junctional communication may be involved in the coordination of cell signaling and migration during morphogenesis of the notochord. Toward the end of gastrulation in wild-type embryos, the axial hypoblast begins morphogenesis into the notochord and creates a visible boundary between the notochordal precursor cells and the paraxial hypoblast. This boundary is not observed in *ntl* mutant embryos even though notochordal precursor cells are still present (Halpern *et al.,* 1993). The inability of the notochordal precursor cells in *ntl* mutant embryos to organize into a morphologically distinct structure correlates with the absence of *Cx43.4* expression in these mutant cells and suggests that *Cx43.4* expression in the notochord is a downstream consequence of Ntl function in the differentiation of the notochord.

floating head (*flh*) mutant embryos also lack notochord, presumably as a result of a cell autonomous shift from a notochordal fate to a somite fate (Halpern *et al.,* 1995; Talbot *et al.,* 1995). The Flh protein, a homeodomain protein, is thought to act in cells upstream of the *ntl* gene product during notochord differentiation, as *flh* mutant embryos show a reduced expression of the *ntl* gene in the axial hypoblast (Talbot *et al.,* 1995). In *flh* mutant embryos *Cx43.4* expression was also reduced in the axial hypoblast through late gastrula stages, and *Cx43.4* expression was lost during early segmentation in cells which normally form notochord (data not shown). The observation that *Cx43.4* expression was lost in notochordal precursor cells at an earlier stage in *ntl* than in *flh* mutant embryos suggests that the early expression of *Cx43.4* in the notochord primordia is regulated, either directly or indirectly, by the Ntl protein. The reduced expression of *Cx43.4* during gastrulation in notochord precursors of *flh* mutant embryos may result from the reduced expression of the *ntl* gene.

The progressively restricted expression of *Cx43.4* in the developing CNS may follow restrictions in cell fate. For example, rhombomeres in the hindbrain are thought to represent somewhat lineage-restricted compartments (Birgbauer and Fraser, 1994). It has been shown that rhombomeres constitute a communication domain, since there is reduced junctional permeability at interrhombomeric boundaries during the development of the chicken hindbrain (Martinez *et al.,* 1992). This suggests that the expression of *Cx43.4* which we see in ventral lateral cells within each rhombomere may be responsible, at least in part, for junctional communication in each rhombomere. Moreover, the cells within each rhombomere were not dye-coupled with cells in the floor plate of the chick hindbrain (Martinez *et al.,* 1992). In a similar manner, the expression of *Cx43.4* in the cells of the zebrafish floor plate may allow coupling of these cells distinct from the coupling of cells in more lateral positions. Thus, *Cx43.4* could create and/or maintain cell–cell communication in the CNS, leading to the establishment and/or maintenance of differentiation of cells in specific domains.

Mechanism for Cx43.4 during Embryogenesis

Cx43.4 may provide for closely linked adhesive and cell communication properties in groups of cells within the zebrafish embryo. This could relate, at least in part, to a role for gap junctions in the establishment and/or maintenance of differences in cell adhesion, migration, and the interpretation of positional values (Meyer *et al.,* 1992; Warner, 1992; Paul *et al.,* 1995). For example, the inability of transplanted *ntl* cells to incorporate into wild-type notochord (Halpern *et al.,* 1993) is similar to the defects in cell adhesion observed when gap junctional communication is inhibited during embryogenesis (Warner *et al.,* 1984; Lee *et al.,* 1987; Bevilacqua *et al.,* 1989; Paul *et al.,* 1995). Studies in mice also support a role for the mouse *T* gene in morphogenetic cell movements and cell adhesion (Wilson *et al.,* 1995). Thus, the role of *Cx43.4* in notochord differentiation may be in the establishment and/or maintenance of cell adhesion. The absence of *Cx43.4* expression in the notochordal

precursor cells of *ntl* mutant embryos may account for the inability of these mutant cells to incorporate into wild-type notochord. Gap junctional communication established by *Cx43.4* expression as a downstream consequence of Ntl function could be one of the driving forces behind the coalescence of notochord precursor cells into the notochord primordium. Once cells are incorporated into the primordium, *Cx43.4* may also coordinate further morphogenesis and signaling within the notochord by providing for the cell-to-cell spread of diffusable molecules. If the GFP-tagged Cx43.4 forms functional gap junctions, it will be possible to test these hypotheses and analyze the effects of ectopic expression of *Cx43.4*, both within specific structures in the living embryo and within the cells which make up those structures.

ACKNOWLEDGMENTS

We thank Drs. M. Halpern, C. Kimmel, and M. Westerfield (University of Oregon) for fish stocks and Drs. K. Helde, R. Riggleman, and D. Grunwald (University of Utah) for the gift of the zebrafish cDNA library. We thank Dr. Truus te Kronnie, M. McGrail, S. Fahrenkrug, Dr. H. J. Yost, and Dr. M. Halpern for useful comments and discussions on the manuscript and the helpful discussions of Dr. R. Riggleman on *in situ* hybridization in zebrafish. We are grateful to M. McGrail for her assistance with confocal microscopy and R. Essner for his help in the establishment and maintenance of our zebrafish facility. J.J.E. was supported by Minnesota Sea Grant USDOC/NA 46RG0101-02 (Paper JR 416) and J.G.L. was supported by a fellowship from the American Heart Association (AHA), MO affiliation. E.C.B. is an Established Investigator of the AHA. This work was supported by NIH Grant R01-RR06625 to P.B.H., NIH Grant HL45466 to E.C.B., and NIH Grant R01-GM46277 to R.G.J.

REFERENCES

Bennett, M. V. L., Barrio, L. C., Bargiello, T. A., Spray, D. C., Hertzberg, E., and Saez, J. C. (1991). Gap junctions: New tools, new answers, and new questions. *Neuron* 6, 305–320.

Bevilacqua, A., Loch-Caruso, R., and Erickson, R. P. (1987). Abnormal development and dye coupling produced by antisense RNA to gap junction protein in mouse preimplantation embryos. *Proc. Natl. Acad. Sci. USA* 86, 5444–5448.

Beyer, E. C. (1990). Molecular cloning and developmental expression of two chick embryo gap junction proteins. *J. Biol. Chem.* 265, 14439–14443.

Beyer, E. C., Paul, D. L., and Goodenough, D. A. (1987). Connexin43: A protein from rat heart homologous to a gap junction protein from liver. *J. Cell Biol.* 105, 2621–2629.

Beyer, E. C., Paul, D. L., and Goodenough, D. A. (1990). Connexin family of gap junction proteins. *J. Membr. Biol.* 116, 187–194.

Birgbauer, E., and Fraser, S. E. (1994). Violation of cell lineage restriction compartments in the chick hindbrain. *Development* 120, 1347–1346.

Boitano, S., Dirksen, E. R., and Sanderson, M. J. (1992). Intercellular propagation of calcium waves mediated by inositol trisphosphate. *Science* 258, 292–295.

Crameri, A., Whitehorn, E. A., Tate, E., and Stemmer, W. P. C. (1996). Improved green fluorescent protein by molecular evolution using DNA shuffling. *Nature Biotech.* 14, 315–319.

Charles, A. C., Naus, C. C., Zhu, D., Kidder, G. M., Dirksen, E. R., and Sanderson, M. J. (1992). Intercellular calcium signaling via gap junctions in glioma cells. *J. Cell Biol.* 118, 195–201.

Danos, M. C., and Yost, H. J. (1995). Linkage of cardiac left-right asymmetry and dorsal-anterior development in *Xenopus*. *Development* 121, 1467–1474.

Darrow, B. J., Laing, J. G., Lampe, P. D., Saffitz, J. E., and Beyer, E. C. (1995). Expression of multiple connexins in culture of neonatal rat cardiac myocytes. *Circ. Res.* 76, 381–387.

Fraser, S. E., Green, C. R., Bode, H. R., and Gilula, N. B. (1987). Selective disruption of gap junctional communication interferes with a patterning process in *Hydra*. *Science* 237, 49–55.

Gevers, P., and Timmermans, L. P. M. (1991). Dye-coupling and the formation and fate of the hypoblast in the teleost fish embryo, *Barbus conchonius*. *Development* 112, 431–438.

Gont, L. K., Steinbeisser, H., Blumberg, B., and De Robertis, E. M. (1993). Tail formation as a continuation of gastrulation: the multiple cell populations of the *Xenopus* tail bud derive from the late blastopore lip. *Development* 119, 991–1004.

Guthrie, S. C. (1984). Patterns of junctional permeability in the early amphibian embryo. *Nature* 311, 149–151.

Halpern, M. E., Ho, R. K., Walker, C., and Kimmel, C. B. (1993). Induction of muscle pioneers and floor plate is distinguished by the zebrafish *no tail* mutation. *Cell* 75, 99–111.

Halpern, M. E., Thisse, C., Ho, R. K., Thisse, B., Riggleman, B., Trevarrow, B., Weinberg, E. S., Postlethwait, J. H., and Kimmel, C. B. (1995). Cell-autonomous shift from axial to paraxial mesodermal development in zebrafish floating head mutants. *Development* 121, 4257–4264.

Hammerschmidt, M., and Nusslein-Volhard, C. (1993). The expression of a zebrafish gene homologous to *Drosophila snail* suggests a conserved function in invertebrate and vertebrate gastrulation. *Development* 119, 1107–1118.

Hennemann, H., Schwarz, H. J., and Willecke, K. (1992). Characterization of gap junction genes expressed in F9 embryonic carcinoma cells: molecular cloning of mouse connexin31 and -45 cDNAs. *Eur. J. Cell Biol.* 57, 51–58.

Kanter, H. L., Saffitz, J. E., and Beyer, E. C. (1992). Cardiac myocytes express multiple gap junction proteins. *Circ. Res.* 70, 438–444.

Kanter, H. L., Laing, J. G., Beyer, E. C., Green, K. G., and Saffitz, J. E. (1993). Multiple connexins colocalize in canine ventricular myocyte gap junctions. *Circ. Res.* 73, 344–350.

Kanter, H. L., Saffitz, J. E., and Beyer, E. C. (1994). Molecular cloning of two human cardiac gap junction proteins, connexin40 and connexin45. *J. Mol. Cell. Cardiol.* 26, 861–868.

Kimmel, C. B., Spray, D. C., and Bennett, M. V. L. (1984). Developmental uncoupling between blastoderm and yolk cell in the embryo of the teleost. *Fundulus. Dev. Biol.* 102, 483–487.

Kimmel, C. B., and Law, R. D. (1985). Cell lineage of zebrafish blastomeres. II. The formation of the yolk syncytial layer. *Dev. Biol.* 108, 86–93.

Kimmel, C. B., Warga, R. M., and Schilling, T. F. (1990). Origin and organization of the zebrafish fate map. *Development* 108, 581–594.

Kimmel, C. B., Ballard, W. W., Kimmel, S. R., Ullmann, B., and Schilling, T. F. (1994). Stages of embryonic development of the zebrafish. *In* ''The Zebrafish Book'' (M. Westerfield, Ed.), pp. 3.27–3.76. Univ. of Oregon Press.

Koval, M., Geist, S. T., Westphale, E. M., Kemendy, A. E., Civitelli,

R., Beyer, E. C., and Steinberg, T. H. (1995). Transfected Connexin45 alters gap junction permeability in cells expressing endogenous Connexin43. *J. Cell Biol.* 130, 987–995.

Kyte, J., and Doolittle, R. F. (1982). A simple method for displaying the hydropathic character of a protein. *J. Mol. Biol.* 157, 105–132.

Laing, J. G., Westphate, E. M., Engelmann, G. L., and Beyer, E. C. (1994). Characterization of the gap junction protein, Connexin45. *J. Membr. Biol.* 139, 31–40.

Lee, S., Gilula, N. B., and Warner, A. E. (1987). Gap junctional communication and compaction during preimplantation stages of mouse development. *Cell* 51, 851–860.

Martinez, S., Geigo, E., Sanchez-Vives, M. V., Puelles, L., and Gallego, R. (1992). Reduced junctional permeability at interrhombomeric boundaries. *Development* 116, 1069–1076.

Mege, R. M., Matsuzaki, F., Gallin, W. J., Goldberg, J. I., Cunningham, B. A., and Edelman, G. M. (1988). Construction of epithelioid sheets by transfection of mouse sarcoma cells with cDNAs for chicken cell adhesion molecules. *Proc. Natl. Acad. Sci. USA* 85, 7274–7278.

Meyer, R. A., Laird, D. W., Revel, J.-P., and Johnson, R. G. (1992). Inhibition of gap junction and adherens junction assembly by connexin and A-CAM antibodies. *J. Cell Biol.* 119, 179–189.

Moon, R. T., and Christian, J. L. (1992). Competence modifiers synergize with growth factors during mesoderm induction and patterning in *Xenopus*. *Cell* 71, 719–712.

Murray, S. A., and Fletcher, W. H. (1984). Hormone-induced intercellular signal transfer dissociates cyclic AMP-dependent protein kinase. *J. Cell Biol.* 98, 1710–1719.

Olson, D. J., Christian, J. L., and Moon, R. T. (1991). Effect of Wnt-1 and related proteins on gap junctional communication in *Xenopus* embryos. *Science* 252, 1175–1176.

Olson, D. J., and Moon, R. T. (1992). Distinct effects of ectopic expression of *Wnt*-1, Activin B, and bFGF on gap junctional permeability in 32-cell *Xenopus* embryos. *Dev. Biol.* 151, 204–212.

Paul, D. L., Yu, K., Bruzzone, R., Gimlich, R. L., and Goodenough, D. A. (1995). Expression of a dominant negative inhibitor of intercellular communication in the early *Xenopus* embryo causes delamination and extrusion of cells. *Development* 121, 371–381.

Prasher, D. C., Eckenrode, V. K., Ward, W. W., Prendergast, F. G., and Cormier, M. J. (1992). Primary structure of the *Aequorea victoria* green-fluorescent protein. *Gene* 111, 229–233.

Puissant, C., and Houdebine, L.-M. (1990). An improvement of the single-step method of RNA isolation by acid guanidinium thiocyanate-phenol-chloroform extraction. *BioTechniques* 8, 148–149.

Reaume, A. G., de Sousa, P. A., Kulkarni, S., Langille, B. L., Zhu, D., Davies, T. C., Juneja, S. C., Kidder, G. M., and Rossant, J. (1995). Cardiac malformation in neonatal mice lacking Connexin43. *Science* 267, 1831–1834.

Ruangvoravat, C. P., and Lo, C. W. (1992). Connexin43 expression in the mouse embryo: localization of transcripts within developmentally significant domains. *Dev. Dyn.* 194, 261–281.

Saez, J. C., Connor, J. A., Spray, D. C., and Bennett, M. V. L. (1989). Hepatocyte gap junctions are permeable to the second messenger, inositol 1,4,5-trisphosphate, and to calcium ions. *Proc. Natl. Acad. Sci. USA* 86, 2708–2712.

Sambrook, J., Fritsch, E. F., and Maniatis, T. (1989). ''Molecular Cloning: A Laboratory Manual,'' 2nd ed. Cold Spring Harbor Laboratory Press, Cold Spring Harbor, New York.

Sanderson, M. J., Charles, A. C., Boitano, S., and Dirksen, E. R. (1994). Mechanisms and function of intercellular calcium signaling. *Mol. Cell Endocrinol.* 98, 173–187.

Schulte-Merker, S., Ho, R. K., Herrmann, B. G., and Nusslein-Volhard, C. (1992). The protein product of the zebrafish homologue of the mouse *T* gene is expressed in nuclei of the germ ring and notochord of the early embryo. *Development* 116, 1021–1032.

Schulte-Merker, S., van Eeden, F. J. M., Halpern, M. E., Kimmel, C. B., and Nusslein-Vohard, C. (1994). *no tail (ntl)* is the zebrafish homologue of the mouse *T* (*Brachyury*) gene. *Development* 120, 1009–1015.

Selman, K., Wallace, R. A., Sarka, A., and Qi, X. (1993). Stages of oocyte development in the zebrafish, *Brachydanio rerio*. *J. Morphol.* 218, 203–224.

Shih, J., and Fraser, S. E. (1995). Distribution of tissue progenitors within the shield region of the zebrafish gastrula. *Development* 121, 2755–2765.

Steinberg, T. H., Civitelli, R., Geist, S. T., Robertson, A. J., Hick, E., Veenstra, R. D., Wang, H.-Z., Warlow, P. M., Westphale, E. M., Laing, J. G., and Beyer, E. C. (1994). Connexin43 and Connexin45 form gap junctions with different molecular permeabilities in osteoblastic cells. *EMBO J.* 13, 744–750.

Sullivan, R., and Lo, C. W. (1995). Expression of a connexin43/β-galactosidase fusion protein inhibits gap junctional communication in NIH3T3 cells. *J. Cell Biol.* 103, 419–429.

Talbot, W. S., Trevarrow, B., Halpern, M. E., Melby, A. E., Farr, G., Postlethwait, J. H., Jowett, T., Kimmel, C. B., and Kimelman, D. (1995). A homeobox gene essential for zebrafish notochord development. *Nature* 378, 150–157.

Thisse, C., Thisse, B., Schilling, T. F., and Postlethwait, J. H. (1993). Structure of the zebrafish *snail1* gene and its expression in wild-type, *spadetail* and *no tail* mutant embryos. *Development* 119, 1203–1215.

Veenstra, R. D., Wang, H.-Z., Beyer, E. C., and Brink, P. R. (1994). Selective dye and ionic permeability of gap junction channels formed by Connexin45. *Circ. Res.* 75, 483–490.

Warga, R. M., and Kimmel, C. B. (1990). Cell movements during epiboly and gastrulation in zebrafish. *Development* 108, 569–580.

Warner, A. (1992). Gap junctions in development—A perspective. *Semin. Cell Biol.* 3, 81–91.

Warner, A. E., Guthrie, S. C., and Gilula, N. B. (1984). Antibodies to gap junctional protein selectively disrupt junctional communication in the early amphibian embryo. *Nature* 311, 127–131.

Westerfield, M. (1993). ''The Zebrafish Book.'' Univ. of Oregon Press.

Wilson, V., Manson, L., Skarnes, W. C., and Beddington, R. S. P. (1995). The T gene is necessary for normal mesodermal morphogenetic cell movements during gastrulation. *Development* 121, 877–886.

Yamada, T., Placzek, M., Tanaka, H., Dodd, J., and Jessell, T. M. (1991). Control of cell pattern in the developing nervous system: polarizing activity of the floor plate and notochord. *Cell* 64, 635–647.

Yancey, S. B., Biswal, S., and Revel, J.-P. (1992). Spatial and temporal patterns of distribution of the gap junction protein connexin43 during mouse gastrulation and organogenesis. *Development* 114, 203–212.

Received for publication January 2, 1996
Accepted May 6, 1996